Optimization of Bio-Orthogonal Non-Canonical Amino acid Tagging (BONCAT) for effective low-disruption labelling of Arabidopsis proteins *in vivo*

Nicholas Hassan[1], Shelly Braun[2], Mohana Talasila[1], Curtis Kennedy[3], Luke Yaremko[3], Richard P. Fahlman[2] and R. Glen Uhrig[1,2#]

[1] Department of Biological Sciences, University of Alberta, Edmonton, Alberta, Canada
[2] Department of Biochemistry, University of Alberta, Edmonton, Alberta, Canada
[3] Department of Computing Science, University of Alberta, Edmonton, Alberta, Canada

[#] Senior and corresponding author:

Dr. R. Glen Uhrig
Department of Biological Sciences,
University of Alberta,
Edmonton, Alberta, Canada, T6G 2E9
Email: ruhrig@ualberta.ca
Phone: +1 780 492 3088
Fax : +1 780 492-9234ruhrig@ualberta.ca

Running Title: Developing Bio-Orthogonal Non-Canonical Amino acid Tagging (BONCAT) for *in-vivo* labelling of newly synthesized plant proteins in plants

Key Words: BONCAT, Click Chemistry, Mass Spectrometry, Quantitative Proteomics

ABSTRACT

Plants require robust responses in protein synthesis to adapt to variable environmental conditions. Measurement of newly synthesized proteins has been successfully facilitated with Bio-Orthogonal Non-Canonical Amino acid Tagging (BONCAT) across a multitude of organisms. Here, we use non-canonical amino acids (NCAAs) L-azidohomoalanine (AHA) or L-homopropargylglycine (HPG) incorporation in place of methionine residues into the actively translating *Arabidopsis* proteome, allowing for that subset of proteins to be enriched for mass spectrometry quantification. Although this technique has seen occasional use in plants, optimization of the protocol to maximize functionality while minimizing organismal stress has not yet been established. Here, we provide evidence for successful implementation through the liquid immersion of seedlings in AHA or HPG-containing media that functions with significantly lower concentrations than the literature standard. Our approach splits acute exposure and incorporation phase of labelling to mitigate potential negative impacts of prolonged NCAA exposure without compromising effective enrichment capacity, and demonstrate that this results in an unperturbed growth phenotype for AHA-treated seedlings. Finally, we demonstrate the capacity of this modified approach to enrich newly synthesized proteins from the whole proteome under standard stress conditions. These improvements allow for a broader use of BONCAT technologies in molecular plant research, affording a deeper understanding of the newly synthesized proteome without negatively impacting plant health.

INTRODUCTION

Balancing protein synthesis and degradation defines proteostasis in all cells, which in turn defines the function of all organisms. Rapid adjustment of protein levels and proteome plasticity is essential for survival in a changing environment, especially for plants, which are carefully tuned to their environmental changes. Defining newly synthesized proteins, or the nascent proteome, is crucial to understanding plant cell regulation and adaptation to environmental stressors. However, conventional strategies for labelling the newly synthesized proteome, such as radiolabelling, lack depth of analysis (Tivendale et al., 2021), while characterization of the nascent proteome by enrichment-based mass spectrometry (MS) approaches can better quantify changes in lower abundant proteins. To fill this niche, Bio-Orthogonal Non-Canonical Amino acid Tagging (BONCAT), has been developed to label nascent proteins with a methionine analog, allowing for enrichment of newly synthesized proteins (Dieterich et al., 2006; Parker and Pratt, 2020).

BONCAT utilizes a combination of azide and alkyne groups to form irreversible conjugations via a copper-catalyzed azide-alkyne cycloaddition (CuAAC; reviewed in Chen et al., 2023). To employ this in a biological setting, unnatural methionine analogs L-azidohomoalanine (AHA, azide) or L-homopropargylglycine (HPG, alkyne) are supplied to live organisms. These non-canonical amino acids (NCAAs) are incorporated into proteins during synthesis by the relatively promiscuous methionine tRNA (Figure 1A; Bagert et al., 2014). Labelled proteins are then extracted and “clicked” to the opposing azide or alkyne conjugated to biotin, effectively biotinylating newly synthesized proteins to facilitate enrichment via streptavidin coupled matrix for subsequent quantification via liquid chromatography (LC)-MS/MS. While BONCAT was initially deployed in mammalian cells, it has since found use in a wide variety of organisms, such as live mice, bacteria, and archaea (Dieterich et al., 2006; Kern and Ferreira-Cerca, 2022; Lindivat et al., 2021; Saleh et al., 2019). However, unlike other organisms, BONCAT implementation in plants has not been fully realized.

In the model plant *Arabidopsis thaliana* (Arabidopsis), BONCAT was first implemented in 2017. Here, AHA and HPG were applied to Arabidopsis seedlings through the flooding of agar plates with 1 mM AHA (Glenn et al., 2017). This yielded thousands of enriched proteins after only a few hours of exposure. However, subsequent endeavours found that Arabidopsis reacts metabolically to NCAAs similar to excess methionine, stunting plant growth and/or impacting plant health during prolonged exposure (Tivendale et al., 2021). Since then, only a handful of studies have utilized BONCAT in plants, with protocol updates generally focused on seedling exposure time to high concentrations of NCAAs (Li et al., 2023; Linster et al., 2022; Lyu et al., 2023; Xie et al., 2023; Yu et al., 2020). Together, these studies indicate that optimization of BONCAT in plants remains

54 incomplete, as a wider variety of experimental parameters need to be tested to strike a balance
55 between effective NCAA labelling concentrations and minimal disturbance plant health.
56 Additionally, protocol simplification efforts remain unexplored, including: a) using the same biotin-
57 conjugated clicked extract for both anti-biotin blots and enrichment for LC-MS/MS analysis to
58 minimize variability and b) exploring the exclusivity of the azide-alkyne cycloaddition, including
59 eliminating the need for repeated precipitation or sample processing prior to remove metabolites
60 prior to "clicking" (Ma et al., 2018).
61 Here, we present an adapted protocol for BONCAT labelling of Arabidopsis seedlings in liquid
62 MS medium that allows for more reliable seedling exposure to, and removal of, AHA and HPG
63 (Figure 1B). Specifically, we demonstrate that the titration of AHA and HPG as well as optimization
64 of labelling time is an effective approach to balance labelling while minimizing exposure to NCAAs.
65 Lastly, we perform extensive seedling viability assays to ensure minimal disruption of plant growth
66 using the modified protocol, and evaluate the newly synthesized proteome using the modified
67 protocol under high and low acute salt and mannitol stress via LC-MS/MS.
68
69 **RESULTS AND DISCUSSION**
70 ***AHA and HPG label Arabidopsis seedlings at 50 µM or less using short application pulses***
71 To determine concentrations of AHA and HPG suitable for application pulses, 5 d-old seedlings
72 were acclimated to liquid medium overnight before being exposed to 0, 10, 25, 50, 100, or 250
73 µM AHA or HPG for 30 min (see Materials and Methods). Washed seedlings were then allowed
74 to incorporate NCAAs into the nascent proteome for an additional 3 h before whole plants were
75 flash frozen and extracted. Copper-catalyzed click chemistry was then performed *in vitro* to
76 conjugate NCAA tags to biotin, and total proteome biotinylation was detected via immunoblot.
77 Anti-biotin immunoblotting against untagged controls was selected as the preferred method for
78 monitoring qualitative labelling efficiency, as whole proteome analysis may not detect AHA tags
79 that have a mass shift similar to salt adducts of methionine (Liu et al., 2022). Here, AHA was found
80 to have the best above-background labelling at all tested concentrations (Figure 2A). Based on
81 these results, a concentration of 50 µM AHA or HPG was selected as an optimal concentration
82 due to clearly visible labelling with minimal required reagent given the known metabolic stress of
83 NCAAs (Tivendale et al., 2021).
84 We then performed time-course labelling to select ideal labelling periods. Labelling periods
85 were divided into acute exposure time (NCAA present in medium) and incorporation time (NCAA
86 removed from medium), with NCAA proteome incorporation assessed independently. This
87 revealed that increased exposure time increases labelling over the course of 24 h at both 50 µM

88 AHA and HPG, with above-background labelling visible within the first 15 min (Figure 2B).
89 Similarly, increased incorporation time with a set initial exposure of 30 min appears to increase
90 labelling for up to 6 h after removal of tags using an initial 50 μM of either NCAA, suggesting
91 residual NCAA likely remains present in the plant's tissues after wash and removal from the
92 medium, with that the remaining reagent continuing to be incorporated for several hours (Figure
93 2C). From this data, a 30 min exposure followed by 3 h of NCAA incorporation were selected as
94 optimal labelling times for 50 μM of either NCAA, with a shorter acute time to mitigate potential
95 negative effects of exposure on the seedlings. Interestingly, concentrations of AHA as low as 10
96 μM also showed increases in labelling across longer exposure times, but labelling stagnated with
97 prolonged incorporation (Figure 2D). Therefore, a NCAA concentration of 10 μM is likely too low
98 for excess NCAA to accumulate in plant tissue prior to its removal, but may be more suitable for
99 long-term exposure labelling, such as overnight incubations for pulse-chase assay.
100
101 ***Short exposure times prevent problems associated with prolonged exposure to AHA***
102 Viability assays of NCAA treated Arabidopsis seedlings was performed by assessing fold-
103 change in root length as a proxy for plant growth, in order to measure the potential negative effects
104 of AHA and HPG. Here, 5 d-old Arabidopsis seedlings were transplanted onto 0.5x MS agar plates
105 containing AHA or HPG and allowed to grow for multiple days. All tested concentrations from 10
106 to 250 μM AHA and HPG decreased plant root growth across a 3-day exposure, with HPG being
107 significantly worse than AHA, even at comparably low concentrations (Figure 3A, Supplemental
108 Figure 1A). However, with only 24 h of exposure, 10 μM AHA did not show a significant reduction
109 in root growth. As this concentration shows above-background labelling within a few hours but
110 does not continue to incorporate the NCAA after being washed (Figure 2D), 10 μM AHA may find
111 an appropriate use in pulse-chase assays, where its capacity for 24-h acute exposure labelling
112 could be used to label plants overnight for degradation experiments the following day.
113 Differing approaches for *in vivo* AHA and HPG viability treatments have been deployed
114 previously. For example, use of 1 mM AHA or HPG to acutely flood Arabidopsis seedlings growing
115 on MS-agar plates revealed a negative impact on whole seedling growth and cell culture viability,
116 in addition to perturbed metabolism (Tivendale et al., 2021). However, other eukaryotes
117 demonstrate a more mixed or neutral response to NCAA exposure. For example, 2 mM AHA and
118 1 mM HPG have no negative viability effects on monkey and mouse-derived cells, while HeLa
119 cells exhibit perturbation responses to AHA that seem to be mitigated by the presence of
120 methionine in the growth medium (Bagert et al., 2014; Su Hui Teo et al., 2016; Wisse et al., 2017).
121 On the molecular level, mouse-derived cell lines exhibit moderate stress signals (e.g. increased

122 HEAT SHOCK PROTEIN 70 and 90 abundance) when treated with 50 μM AHA, but no significant
123 increase in global protein ubiquitination and/or apoptosis/cell death associated with a reduction in
124 viability (Morey et al., 2021).
125 In contrast, Tivendale et al. (2021) found AHA to be more toxic than HPG, especially in plant
126 cell cultures. Bacteria have shown similar concentration-dependent sensitivity to NCAAs, but in a
127 manner more consistent with this study. AHA appears to be tolerable to log-phase *E. coli* at higher
128 concentrations than HPG, where HPG reduced bacterial growth at concentrations above 2.8 μM
129 while AHA was tolerated up to the 200 μM range for prolonged exposure (Landor et al., 2023).
130 This effect differs slightly between prototrophs and auxotrophs, where bacteria unable to
131 synthesize essential compounds appear to be more negatively affected by HPG (Jecmen et al.,
132 2023). Both AHA and HPG mildly affect bacterial metabolism as well, but are not degraded as the
133 expected products of methionine (Steward et al., 2020).
134 It has been proposed that negative long-term effects of NCAAs on organism or cell growth may
135 be irrelevant if incorporation into nascent proteins and immediate toxicity does not occur during
136 the length of the experiment (Landor et al., 2023). To date, viability assays in plants have
137 examined organism or cellular responses over prolonged exposure times, which is not always
138 representative of the experimental conditions. Therefore, we repeated viability assays with a more
139 representative exposure (short acute exposure in liquid 0.5x MS), followed by seedling washing
140 and return to 0.5x MS - agar plates. All tested concentrations of AHA (up to 250 μM) did not reduce
141 plant growth compared to controls after a 30-min AHA exposure (Figure 3B-C, Supplemental
142 Figure 1B), suggesting that the long-term exposure growth defects are not a result of immediate
143 toxicity of the NCAA. In contrast, 50 μM and 100 μM concentrations of HPG showed a slight
144 reduction in growth compared to control under the same conditions (Figure 3C). By limiting
145 exposure to 30 min and allowing incorporation to continue for < 6 h, viability concerns can be
146 avoided without compromising in labelling efficiency, particularly in the use case of AHA. To strike
147 a balance in labelling efficiency while minimising potential toxicity, the experimental settings for
148 stress experimentation were set as 30 minutes of direct exposure to 50μM AHA, followed by 3
149 hours of incorporation time, and harvesting.
150
151 ***AHA-labelled proteins under salt and osmotic stress***
152 To benchmark the quantitative labelling efficiency of the optimized protocol under different
153 experimental conditions, we applied two abiotic stress conditions during AHA labelling to compare
154 conditions known to have overlapping, but not fully redundant, effects on the plant proteome
155 (Rodriguez Gallo et al., 2023). The experiment was performed with either ‘high stress’ (150 mM

156 salt or 300 mM mannitol) or 'low stress' (50 mM salt or 100 mM mannitol) conditions, as the effects
157 of applied stressors may be intensified by liquid submersion. All stressors were applied for the
158 entire duration of exposure and incorporation treatment (3 hours). Here, we find 549 proteins
159 enriched in at least one condition under high stress conditions, 797 under low stress conditions,
160 with a greater percentage of overlapping proteins between groups under lower stress versus high
161 stress (55.1% vs. 35.1%; Figure 4A). Hundreds of these proteins represent Class I hits, which we
162 define as below detection in the MS2 spectra of negative control samples (Figure 4B). Further
163 principal component analyses found AHA-treated samples cluster away from untreated (bead
164 binding control) samples, but distance between clusters of stressed and unstressed samples vary
165 with abiotic stress intensity (Figure 5A and B).
166 Additionally, using positive AHA-labeled control samples, we can disentangle stress specific
167 responses. Network analysis of dynamically changing salt and mannitol responsive proteins,
168 resolved multiple protein networks related to abiotic stimulus response (Figure 4C). Gene
169 ontology (GO) enrichment analysis further validated enrichment of abiotic stress response
170 biological processes under the stress conditions, including wax biosynthesis and water-related
171 regulation (Figure 4D, Supplemental Figure 2, Supplemental Figure 3). Consistent with prior
172 findings, responses to salt and mannitol at the protein level appear to differ from each other
173 (Supplemental Figure 4; Rodriguez Gallo et al., 2023) Next, we compared our BONCAT
174 enrichment data to the changing salt and osmotic proteome resolved by Rodriguez Gallo et al.
175 (2023). While BONCAT enrichment resolves overall fewer significantly changing proteins, we find
176 hundreds of proteins in our BONCAT enrichment data stress conditions that were also significantly
177 changing in the stress data of Gallo and colleagues (2023), including known salt and osmotic
178 responsive CALCIUM-DEPENDENT PROTEIN KINASE 6 (AtCDPK6; Xu et al., 2010) and
179 osmotic stress responsive RNA-binding protein ALDEHYDE DEHYDROGENASE 7B4
180 (AtALDH7B4; Figure 4C, Supplemental Figure 5A, Marondedze et al., 2019). We also find more
181 than 100 proteins that while significantly enriched in our data under stress conditions that do not
182 exhibit a significant change in their whole proteome abundance, despite gene ontology showing
183 their involvement in abiotic stress (Rodriguez Gallo et al., 2023, Supplemental Figure 5B,
184 Supplemental Figure 6). This indicates that BONCAT provides abiotic stress induced protein
185 production response information that cannot be achieved through conventional whole proteome
186 analyses, offering a more nuanced understanding of abiotic stress response relative to whole
187 proteome analysis alone.
188

189 ***BONCAT isolates newly produced proteins and proteins eluding quantification by whole***
190 ***proteome analyses***
191 An advantage of BONCAT is the ability to observe proteins that may be degraded and
192 produced at similar rate, or proteins produced in low abundance, both of which would go unnoticed
193 in conventional total proteome analysis. To examine this scenarios, we examined comparable
194 AHA-labeled and untreated control whole seedling proteomes to determine if there is a detectable
195 effect of the amino acid analog treatment at the molecular level and to compare the proteins found
196 in AHA-labelled whole proteome versus BONCAT enriched samples. Of the more than 8000
197 proteins quantified in the whole proteome, only 208 were significantly different between AHA-
198 treated and untreated control samples (~2.5%; *q-value* < 0.05), with only 15 of those significant
199 proteins detected in the AHA enriched sample set of 628 (~2.3%; Figure 5C), indicating at low
200 concentrations AHA elicits minimal molecular perturbations. Furthermore, of the 628 AHA-treated
201 proteins enriched without added stress conditions, we quantified 501 to not be significantly
202 changing in the whole proteome, indicating that AHA labelling is precisely detecting the production
203 of new proteins. Additionally, 111 of the 628 BONCAT-enriched proteins are not detected in the
204 whole proteome analysis, indicating click-based enrichment allows detection of newly synthesized
205 proteins that are low in abundance. Lastly, we examined our click-enriched proteins for bias
206 towards methionine rich proteins (Figure 5D). Here, no bias for methionine rich proteins relative
207 to the Arabidopsis proteome was found. Collectively, these results further indicate that we are
208 enriching for proteins that are produced in response to salt stress.
209
210 **SUMMARY**
211 In this study, we established a simple and usable workflow for the implementation of BONCAT
212 in plants. Although 50 µM AHA was selected as the optimal labelling concentration, the protocol
213 is flexible and modifiable based on need, with modified protocols able to be tracked for efficiency
214 at multiple stages. Our BONCAT implementation showed an ability clearly define stress and
215 unstressed conditions in relatively short periods that mitigates potential negative plant responses.
216 This unveils outstanding new opportunities for applications where enrichment of a subsect of the
217 proteome is required for sufficient depth of analysis. Lastly, the potential for NCAA-tag
218 incorporation at concentrations substantially below the literature standard has positive new
219 implications for the use of BONCAT in plants moving forward.
220
221 **MATERIALS AND METHODS**
222 ***Plant growth conditions***

223 *Arabidopsis thaliana* seeds (Col-0) were liquid sterilized by immersion in 70% (v/v) ethanol for
224 2 min followed by 30% (v/v) bleach for 10 min. Sterilized seeds were vernalized in H_2O in the dark
225 at 4°C for 3 d. Germination plates were prepared using half-strength MS basal salts (Caisson
226 Laboratories Inc. Murashige & Skoog MSP01), pH adjusted to 5.8 with aqueous KOH, with 0.08%
227 (w/v) agar (Caisson laboratories Inc. Phytoblend PTP01).
228 For click chemistry, vernalized seeds were stratified on plates and allowed to grow with plates
229 positioned vertically in 24 h light at 22°C for 5 days. Approximately 100 mg of 5 d-old seedlings
230 were immersed in autoclaved half-strength MS media in 24-well plates and placed under constant
231 light for 16 h to acclimatize. MS media was removed and replaced with 50 μM filter sterilized L-
232 azidohomoalanine or L-homopropargylglycine (Vector Labs, CCT-1066 and CCT-1076) from 0.1
233 M stocks dissolved in H_2O and diluted in 0.5x MS media. Seedlings were then incubated for 30
234 min of exposure time in constant light before being washed once in 0.5x MS and incubated in
235 constant light in 0.5x MS for 3 hours of "incorporation" time. Stress experiments included either
236 salt (150mM in 'high stress' and 50mM in 'low stress' conditions) or mannitol (300mM in 'high
237 stress' and 100mM in 'low stress' conditions) in the 0.5X MS liquid media during both exposure
238 and incorporation phases. Labelled seedlings were removed from media, rinsed in 0.5x MS, and
239 quickly touch dried before being flash frozen in liquid N_2 and stored at -80°C until subsequent
240 steps.
241 To perform root length assays, seeds were sown individually on 0.5x MS agar plates positioned
242 vertically in dark boxes with seeds at the light interface to emulate roots growing in the dark and
243 shoots growing in the light. Seedling growth conditions consisted of a 12 h photoperiod, 22°C and
244 100 μmol/m^{2}s light. After 5 d for the long-term reagent exposure, seedlings were transplanted
245 along the same light/dark interface to 0.5x MS plates containing 0, 10, 25, 50, or 250 μM AHA or
246 HPG. For the short-term exposure, seedlings were placed into liquid 0.5x MS overnight to
247 equilibrate, then immersed for 30 min in 0.5x liquid MS containing 0, 10, 25, 50, or 250 μM AHA,
248 before being washed in 0.5x MS and re-plated on to vertical plates. Root length was recorded for
249 7 d using digital calipers, and fold-change in individual seedling root length relative to day 0
250 (transplanting day) was plotted. Recording of root length stopped after day 3 for the long-term
251 exposure due to statistically significant differences between all concentrations relative to controls.
252
253 ***Optimization of plant labelling***
254 To determine optimal concentrations of label, variable concentrations of 10, 25, 50, 100, or 250
255 μM of AHA or HPG were applied as above. Optimal concentrations for labelling were chosen
256 based on a combination of intensity of labelled protein present on streptavidin immunoblots and

257 minimal observed growth retardation on 0.5x MS agar containing the same concentration of label.
258 For time-course experimentation, acute exposure times were varied between 15 min, 30 min, or
259 1, 2, 4, or 22 h. Incorporation times were varied between 30 minutes or 1, 2, 3, 6, or 24 h. Optimal
260 incubation times were chosen based on minimal required times to achieve effective labelling at
261 the desired concentration as visualized via immunoblot, and verified to cause insignificant or no
262 growth inhibition to the seedlings based on viability studies.
263
264 ***Protein extraction and quantification***
265 Flash frozen tissue was ground using Geno/Grinder (SPEX SamplePrep) for 30 s at 1200 rpm
266 with 3mm glass beads and extracted in either 50mM HEPES (pH 7.5) with 1% (w/v) SDS or 50
267 mM Tris (pH 8.0) with 1% (w/v) SDS, at a ratio of 1:2 w/v ground tissue to extraction buffer.
268 Following optimization, HEPES was selected as the extraction buffer for all samples due to better
269 click labelling observed. Samples were heated at 95°C for 10 min and 1000 rpm on Eppendorf
270 ThermoMixer F2.0, cooled, and centrifuged at 16,000 xg for 10 min at room temperature to
271 remove tissue particulates. Protein amounts were quantified using Bradford assay with samples
272 diluted to 0.2% (w/v) SDS against BSA controls.
273
274 ***Click chemistry reaction***
275 A total of 250 µg of protein from each sample was diluted in extraction buffer with 1% (w/v) or
276 no SDS to a volume of 346 µL ensuring a final concentration of 0.5% (w/v) SDS to maintain protein
277 solubility. To each reaction, the following was added: 8 µL of 50 mM tris(2-carboxyethyl)phosphine
278 (TCEP)-HCl (Sigma Cat. No: 51805-45-9; diluted from 1 M stock in H_2O same day of use), 30 µL
279 of 1.7 mM tris[(1-benzyl-1H-1,2,3-triazol-4-yl)methyl]amine (TBTA) (Vector Labs Cat. No: CCT-
280 1061; in 20% (v/v) dimethyl sulfoxide (DMSO) and 80% (v/v) tert-butanol, stored at room
281 temperature as in Ma et al., 2018Ma et al., 2018), 8 µL of CuSO4 (Sigma Cat. No: 451657-10G;
282 in H_2O, stored at -20°C), and 8 µL of 5mM biotin-PEG3-azide (Vector Labs Cat. No: CCT-AZ104;
283 for HPG samples, in DMSO) or biotin-PEG4-alkyne (Vector Labs Cat. No: CCT-TA105; for AHA
284 samples, in DMSO). Click reactions were allowed to proceed for 1 h at room temperature, shaking
285 at 700 rpm and protected from light. Reactions were then quenched via chelation with 20 µL of
286 0.5 M ethylenediaminetetraacetic acid (EDTA) (pH 8.0, stored at 4°C). Labelling validation was
287 determined via streptavidin immunoblot using 6 µg of protein run on 10% SDS-PAGE gels
288 transferred to 0.45 µM polyvinylidene fluoride (PVDF) membrane. Blots were blocked in 5% fat-
289 free milk in Tris-buffered saline (TBS) for 1 h, at which point HRP-conjugated streptavidin (Thermo
290 Scientific Cat. No. N100) diluted 1:2000 in Tris-buffered saline with 0.1% Tween-20 (TBST) was

291 added for an additional hour. Membranes were washed in TBST and visualized using Clarity
292 Western ECL Substrate (Bio-Rad Cat No. 170-5060). Colloidal Coomassie Blue-stained gels were
293 used as loading controls.
294
295 ***Enrichment of clicked proteins***
296 Excess biotin and small molecules were removed from clicked samples using Cytiva PD
297 Spintrap G-25 columns (Cat. No: 28918004). Samples were bound to Cytiva streptavidin
298 Sepharose beads (Cytiva Cat. No. 17511301); all depicted experiments proceeded using non-
299 magnetic Sepharose beads. All beads were initially washed 3 times in 50 mM HEPES, pH 7.5, for
300 1 min while rotating at room temperature. For all steps, supernatant was removed by
301 centrifugation for 1 min at 600 xg. Up to 200 µg of flow-through protein from the Spintrap columns
302 was loaded onto equilibrated streptavidin beads and allowed to bind while rotating for 16 hours at
303 4°C. The supernatant was removed and retained at -20°C to assess capture efficiency. A total of
304 4 biological replicates were enriched in each experimental condition.

305 Capture efficiency was checked before digestion via streptavidin-detected dot blot comparison
306 of clicked protein, Spintrap column flow-through, and supernatant after overnight bead binding.
307 After confirmation of a signal reduction of more than 70% in the supernatant after binding, beads
308 were washed sequentially with the following solutions at 1mL each: 50 mM HEPES pH 7.5 (2x
309 washes), 1 M potassium chloride, ice-cold 100 mM sodium carbonate (2x washes), 2 M urea in
310 50 mM Tris-HCl pH 8.0 (2x wash), and 50 mM triethylammonium bicarbonate (TEAB; Sigma Cat.
311 No: 15715-58-9) in HPLC-grade water (3x washes). All washes were completed at room
312 temperature with rotation for 3 min.

313 ***Trypsin digestion and peptide processing***
314 *Enriched Proteome* - Peptides were generated through on bead digestion using sequencing
315 grade trypsin (V5113; Promega) diluted 1:100 in 50 mM TEAB overnight at 37°C; the supernatant
316 was removed before the beads were washed with 50 mM TEAB and the supernatant pooled with
317 previously extracted peptides. The extract was reduced with 10 mM DTT at 95°C for 5 min while
318 shaking at 450 rpm, alkylated with 30 mM iodoacetamide (IA) at room temperature for 30 min,
319 and the reaction quenched with 10 mM DTT for 10 minutes. Samples were then acidified to 0.5%
320 (v/v) TFA to a pH of less than 2 and centrifuged at 16,000 xg for 1 min before the supernatant was
321 removed and dried down. Peptides were re-suspended in 3% (v/v) acetonitrile / 0.1% (v/v) formic
322 acid for desalting via ZipTip (Sigma Cat. No. ZTC18S960) before being dried and stored at -80°C.

323 Desalted peptides were the re-suspended in 3% (v/v) acetonitrile / 0.1% (v/v) formic acid for mass
324 spectrometry analysis.
325 *Whole Proteome* - 100 µg of Arabidopsis seedling protein extracts were generated as
326 previously described without deviation (Rodriguez Gallo et al. 2023). Samples were then digested
327 and processed as described above.
328
329 ***LC MS/MS and Data Analysis***
330 Peptides were analyzed using a FAIMSpro mounted Fusion Lumos Orbitrap mass
331 spectrometer (Thermo Fisher Scientific) in data independent acquisition (DIA) mode. Peptides
332 were injected using Easy-nLC 1200 system (LC140; Thermo Fisher Scientific) and an Acclaim
333 PepMap 100 C18 trap column (Cat# 164750; Thermo Fisher Scientific) followed by a 50 cm Easy-
334 Spray PepMap C18 analytical column (ES903; Thermo Fisher Scientific) warmed to 50 °C.
335 Peptides were eluted at 0.3 µl/min using a segmented solvent B gradient of 0.1% (v/v) formic acid
336 in 80% (v/v) acetonitrile from 4 to 41% solvent B (0–60min). The FAIMSpro was used with a fixed
337 gas flow of 3.5 L/min with a 3-CV setting of -30, -50, -70. A positive ion spray voltage of 2.3 kV
338 was used with an ion transfer tube temperature of 300 °C and an RF lens setting of 40%. Direct
339 DIA acquisition was performed as previously described (Mehta et al., 2022) . Full scan
340 MS^1 spectra (350–1400 *m*/*z*) were acquired with a resolution of 120,000 at 200 *m*/*z* with a
341 normalized automatic gain control (AGC) target of 100% and IT set to automatic. Fragment
342 spectra were acquired at resolution of 30,000 across 28 38.5 *m*/*z* windows overlapping by
343 1 *m*/*z* using a dynamic maximum injection time and an AGC target value of 2000%, with a
344 minimum number of desired points across each peak set to 6. Higher-energy collisional
345 dissociation fragmented was performed using a fixed 27% fragmentation energy. Downstream
346 data analysis of dDIA acquisitions was performed using Spectronaut ver. 19 (Biognosys AG) with
347 default settings as previously described (Mehta et al., 2022) , with all searches made against a
348 custom-made decoy (reversed) version of the Arabidopsis protein database from Araport 11
349 (27,533 protein encoding genes; ver. 2022-09-14). Briefly, search parameters included the
350 following: trypsin digest permitting two missed cleavages, fixed modifications (carbamidomethyl
351 (C)), variable modifications (oxidation (M)) and a peptide spectrum match, peptide and protein
352 false discovery threshold of 0.01.
353
354 ***Bioinformatic Data Analysis***
355 Significantly changing proteins (Log_2FC of MS2 spectra > 0.58 over negative control) were
356 pooled with Class I protein hits (absent in MS2 of negative controls) to form the foreground with

a background of all identified proteins (Supplemental Table 1, Supplemental Table 2). Comparison to whole proteome analysis was done to both AHA-treated unstressed whole proteomes that followed the same standards for analysis (Supplemental Table 3) and previous work on salt and mannitol stressed whole proteomes by Rodriguez Gallo et al. (2023; Supplemental Table 4). Gene Ontology (GO) enrichments were performed using the Ontologizer (Bauer et al., 2008; http://ontologizer.de/, Supplemental Table 5, Supplemental Table 6) using a Benjamini-Hochberg parent-child union with an analysis cutoff of $p > 0.01$, and visualized in R 4.5.0. Proteins below differential abundance in both positive and negative controls was used for network analysis of stress-exclusive proteins via the StringApp plugin for Cytoscape v. 3.10.3, with an edge score cut-off of 0.5 (Doncheva et al., 2019, https://cytoscape.org/). STRING Enrichment using *StringApp* was used to assign gene ontologies. Methionine content analysis was done using in-house Python scripts to analysis methionine content and length of the Arabidopsis protein database from Araport 11 (https://phytozome-next.jgi.doe.gov/ ; Supplemental Table 7). PCA analysis was performed using *SRplot* (Tang et al., 2023), with other visualizations produced using a combination of *ggplot2*, Biorender (https://www.biorender.com/), GraphPad Prism v. 8.4.3 (https://www.graphpad.com/), and Affinity Designer v. 1.10.5 (https://affinity.serif.com/en-us/designer/).

ACKNOWLEDGEMENTS

The authors would like to thank the Canadian Foundation for Innovation (CFI) and Natural Sciences and Engineering Council of Canada (NSERC) for funding this work. We would also like to thank Jack Moore and the Alberta Proteomics and Mass Spectrometry Facility (APM) for mass spectrometry assistance and upkeep.

AUTHOR CONTRIBUTIONS

Nicholas Hassan: Investigation, Conceptualization, Methodology, Data curation, Formal analysis, Visualization, Writing—original draft. *Shelly Braun*: Writing—review & editing, Conceptualization. *Mohana Talasila*: Formal analysis, Data curation, Visualization. *Curtis Kennedy*: Data curation, Visualization. *Luke Yaremko*: Formal analysis, Data curation, Visualization. *Richard Fahlman*: Supervision, Writing—review & editing, Material Resources. *R. Glen Uhrig*: Supervision, Conceptualization, Writing—review & editing, Funding acquisition.

DATA AVAILABILITY

Raw data have been deposited to the ProteomeExchange Consortium (http://proteomecentral.proteomexchange.org) *via* the PRoteomics IDEntification Database (PRIDE; https://www.ebi.ac.uk/pride/) partner repository with the data set identifiers PXD064210

REFERENCES

Bagert, J.D., Xie, Y.J., Sweredoski, M.J., Qi, Y., Hess, S., Schuman, E.M., Tirrell, D.A., 2014. Quantitative, time-resolved proteomic analysis by combining bioorthogonal noncanonical amino acid tagging and pulsed stable isotope labeling by amino acids in cell culture. Molecular and Cellular Proteomics 13, 1352–1358. https://doi.org/10.1074/mcp.M113.031914

Chen, M.M., Kopittke, P.M., Zhao, F.J., Wang, P., 2023. Applications and opportunities of click chemistry in plant science. Trends Plant Sci 29, 167–178. https://doi.org/10.1016/j.tplants.2023.07.003

Dieterich, D.C., Link, A.J., Graumann, J., Tirrell, D.A., Schuman, E.M., Sharpless, K.B., 2006. Selective identification of newly synthesized proteins in mammalian cells using bioorthogonal noncanonical amino acid tagging (BONCAT). National Academy of Sciences 103, 9482–9487.

Doncheva, N.T., Morris, J.H., Gorodkin, J., Jensen, L.J., 2019. Cytoscape StringApp: Network Analysis and Visualization of Proteomics Data. J Proteome Res 18, 623–632. https://doi.org/10.1021/acs.jproteome.8b00702

Gallo, M.C.R., Li, Q., Talasila, M., Uhrig, R.G., 2023. Quantitative Time-Course Analysis of Osmotic and Salt Stress in Arabidopsis thaliana Using Short Gradient Multi-CV FAIMSpro BoxCar DIA. Molecular and Cellular Proteomics 22. https://doi.org/10.1016/j.mcpro.2023.100638

Glenn, W.S., Stone, S.E., Ho, S.H., Sweredoski, M.J., Moradian, A., Hess, S., Bailey-Serres, J., Tirrell, D.A., 2017. Bioorthogonal noncanonical amino acid tagging (BONCAT) enables time-resolved analysis of protein synthesis in native plant tissue. Plant Physiol 173, 1543–1553. https://doi.org/10.1104/pp.16.01762

Jecmen, T., Tuzhilkin, R., Sulc, M., 2023. Photo-Methionine, Azidohomoalanine and Homopropargylglycine Are Incorporated into Newly Synthesized Proteins at Different Rates and Differentially Affect the Growth and Protein Expression Levels of Auxotrophic and Prototrophic E. coli in Minimal Medium. Int J Mol Sci 24. https://doi.org/10.3390/ijms241411779

Kern, M., Ferreira-Cerca, S., 2022. Differential Translation Activity Analysis Using Bioorthogonal Noncanonical Amino Acid Tagging (BONCAT) in Archaea. Ribosome Biogenesis: Methods and Protocols 229–246. https://doi.org/10.1007/978-1-0716-2501-9_14

Landor, L.A.I., Bratbak, G., Larsen, A., Tjendra, J., Våge, S., 2023. Differential toxicity of bioorthogonal non-canonical amino acids (BONCAT) in Escherichia coli. J Microbiol Methods 206. https://doi.org/10.1016/j.mimet.2023.106679

430 Li, X., Chai, X., Lyu, H.N., Fu, C., Tang, H., Shi, Q., Wang, J., Xu, C., 2023. Chemical
431 proteomics reveals an ISR-like response elicited by salicylic acid in Arabidopsis. New
432 Phytologist. https://doi.org/10.1111/nph.18646

433 Lindivat, M., Bratbak, G., Larsen, A., Hess-Erga, O.K., Hoell, I.A., 2021. Flow Cytometric
434 Analysis of Bacterial Protein Synthesis: Monitoring Vitality After Water Treatment.
435 Front Microbiol 12. https://doi.org/10.3389/fmicb.2021.772651

436 Linster, E., Forero Ruiz, F.L., Miklankova, P., Ruppert, T., Mueller, J., Armbruster, L., Gong,
437 X., Serino, G., Mann, M., Hell, R., Wirtz, M., 2022. Cotranslational N-degron masking
438 by acetylation promotes proteome stability in plants. Nat Commun 13.
439 https://doi.org/10.1038/s41467-022-28414-5

440 Liu, C., Wong, N., Watanabe, E., Hou, W., Biral, L., Decastro, J., Mehdipour, M., Aran, K.,
441 Conboy, M.J., Conboy, I.M., 2022. Mechanisms and Minimization of False Discovery
442 of Metabolic Bioorthogonal Noncanonical Amino Acid Proteomics. Rejuvenation Res
443 25, 95–109. https://doi.org/10.1089/rej.2022.0019

444 Lyu, H.N., Fu, C., Chai, X., Gong, Z., Zhang, J., Wang, Jiaqi, Wang, Jigang, Dai, L., Xu, C.,
445 2023. Systematic thermal analysis of the Arabidopsis proteome: Thermal tolerance,
446 organization, and evolution. Cell Syst 14, 883-894.e4.
447 https://doi.org/10.1016/j.cels.2023.08.003

448 Ma, Y., McClatchy, D.B., Barkallah, S., Wood, W.W., Yates, J.R., 2018. Quantitative
449 analysis of newly synthesized proteins. Nat Protoc 13, 1744–1762.
450 https://doi.org/10.1038/s41596-018-0012-y

451 Marondedze, C., Thomas, L., Gehring, C., Lilley, K.S., 2019. Changes in the Arabidopsis
452 RNA-binding proteome reveal novel stress response mechanisms. BMC Plant Biol 19.
453 https://doi.org/10.1186/s12870-019-1750-x

454 Mehta, D., Scandola, S., Uhrig, R.G., 2022. BoxCar and Library-Free Data-Independent
455 Acquisition Substantially Improve the Depth, Range, and Completeness of Label-Free
456 Quantitative Proteomics. Anal Chem 94, 793–802.
457 https://doi.org/10.1021/acs.analchem.1c03338

458 Morey, T.M., Esmaeili, M.A., Duennwald, M.L., Rylett, R.J., 2021. SPAAC Pulse-Chase: A
459 Novel Click Chemistry-Based Method to Determine the Half-Life of Cellular Proteins.
460 Front Cell Dev Biol 9. https://doi.org/10.3389/fcell.2021.722560

461 Parker, C.G., Pratt, M.R., 2020. Click Chemistry in Proteomic Investigations. Cell 180, 605–
462 632. https://doi.org/10.1016/j.cell.2020.01.025

463 Saleh, A.M., Jacobson, K.R., Kinzer-Ursem, T.L., Calve, S., 2019. Dynamics of Non-
464 Canonical Amino Acid-Labeled Intra- and Extracellular Proteins in the Developing
465 Mouse. Cell Mol Bioeng 12, 495–509. https://doi.org/10.1007/s12195-019-00592-1

466 Steward, K.F., Eilers, B., Tripet, B., Fuchs, A., Dorle, M., Rawle, R., Soriano, B.,
467 Balasubramanian, N., Copié, V., Bothner, B., Hatzenpichler, R., 2020. Metabolic
468 Implications of Using BioOrthogonal Non-Canonical Amino Acid Tagging (BONCAT)
469 for Tracking Protein Synthesis. Front Microbiol 11.
470 https://doi.org/10.3389/fmicb.2020.00197

Su Hui Teo, C., Serwa, R.A., O'Hare, P., 2016. Spatial and Temporal Resolution of Global Protein Synthesis during HSV Infection Using Bioorthogonal Precursors and Click Chemistry. PLoS Pathog 12. https://doi.org/10.1371/journal.ppat.1005927

Tang, D., Chen, M., Huang, X., Zhang, Guicheng, Zeng, L., Zhang, Guangsen, Wu, S., Wang, Y., 2023. SRplot: A free online platform for data visualization and graphing. PLoS One 18. https://doi.org/10.1371/journal.pone.0294236

Tivendale, N.D., Fenske, R., Duncan, O., Millar, A.H., 2021. In vivo homopropargylglycine incorporation enables sampling, isolation and characterization of nascent proteins from Arabidopsis thaliana. The Plant Journal 107, 1260–1276. https://doi.org/https://doi.org/10.1111/tpj.15376

Wisse, L.E., Penning, R., Zaal, E.A., van Berkel, C.G.M., ter Braak, T.J., Polder, E., Kenney, J.W., Proud, C.G., Berkers, C.R., Altelaar, M.A.F., Speijer, D., van der Knaap, M.S., Abbink, T.E.M., 2017. Proteomic and metabolomic analyses of vanishing white matter mouse astrocytes reveal deregulation of ER functions. Front Cell Neurosci 11. https://doi.org/10.3389/fncel.2017.00411

Xie, Z., Zhao, S., Li, Ying, Deng, Y., Shi, Y., Chen, X., Li, Yue, Li, H., Chen, C., Wang, X., Liu, E., Tu, Y., Shi, P., Tong, J., Gutierrez-Beltran, E., Li, J., Bozhkov, P. V., Qian, W., Zhou, M., Wang, W., 2023. Phenolic acid-induced phase separation and translation inhibition mediate plant interspecific competition. Nat Plants 9, 1481–1499. https://doi.org/10.1038/s41477-023-01499-6

Xu, J., Tian, Y.S., Peng, R.H., Xiong, A.S., Zhu, B., Jin, X.F., Gao, F., Fu, X.Y., Hou, X.L., Yao, Q.H., 2010. AtCPK6, a functionally redundant and positive regulator involved in salt/drought stress tolerance in Arabidopsis. Planta 231, 1251–1260. https://doi.org/10.1007/s00425-010-1122-0

Yu, H., Kong, X., Huang, H., Wu, W., Park, J., Yun, D.J., Lee, B. ha, Shi, H., Zhu, J.K., 2020. STCH4/REIL2 Confers Cold Stress Tolerance in Arabidopsis by Promoting rRNA Processing and CBF Protein Translation. Cell Rep 30, 229-242.e5. https://doi.org/10.1016/j.celrep.2019.12.012

501 **FIGURES**

502 **Figure 1. Visualization of BONCAT technology.** A) Incorporation mechanism of AHA and HPG
503 into the nascent proteome. B) Workflow for click labelling. Whole seedlings are acclimatized to
504 liquid 0.5X MS media for 24 hours before treatment with AHA or HPG. Acute exposure time in the
505 modified protocol is limited to 30 minutes, followed by 3 hours of incorporation time. Protein is
506 extracted from seedlings for click chemistry in vitro, followed by visualization via anti-biotin blot to
507 determine qualitative labelling before streptavidin enrichment for LC-MS/MS.

508 **Figure 2. Streptavidin-detected anti-biotin blots of biotin-clicked Arabidopsis whole lysate**
509 **samples.** Beneath each blot is a cropped segment of a Coomassie Blue gel loading control. Each
510 experiment was performed in triplicate, but single replicates are shown for simplicity. A) Titration
511 of AHA and HPG concentrations with a 30-minute acute exposure and 3-hour incorporation time.
512 B) 50μM AHA and HPG tested with exposure times varying from 15 minutes to 22 hours, all
513 followed by a 3-hour incorporation. C) 50μM AHA and HPG tested with incorporation times varying
514 from 30 minutes to 24 hours, each preceded with a 30-minute exposure time. D) Low
515 concentration AHA (10μM) test of varying incorporation times with a 30-minute exposure (left) or
516 varying exposure times with a 3-hour incorporation (right).

517 **Figure 3. Viability assays of Arabidopsis seedlings exposed to methionine analogs.**
518 Average fold change in root length of seedlings with standard deviation error bars is plotted, and
519 t-tests between experimental and control groups were performed with p-value significance < 0.05
520 shown. A) n = 72 5 d (days)-old seedlings per condition were transplanted to agar plates
521 containing AHA or HPG for 1-3 d to simulate extensive exposure times. High concentrations after
522 3 days (left), low concentrations after 3 days (middle) and low concentrations after 24 hours (right)
523 are shown. B) n = 54 seedlings per condition were acclimatized to liquid media for 24 h, then
524 exposed for 30 min in AHA- or HPG-containing liquid media before being returned to solid medium
525 and grown for 7 d. C) Snapshot of days 5 and 7 for all conditions from summarized data in 2B to
526 show significant changes.

527 **Figure 4. Mass spectrometry data for 50 μM AHA-labelled 3-hour salt or mannitol stressed**
528 **Arabidopsis seedlings.** A) Upset plot of enriched (>1.5 FC or below detection in negative
529 control) protein groups and overlap between positive control (AHA treated, unstressed) and stress
530 conditions in either high stress (150mM salt and 300mM mannitol, dark, n = 549) or low stress
531 (50mM salt, 100mM mannitol, light, n = 797) conditions. B) Exclusive Class I hits from A that are
532 absent in negative controls (n = 147 high stress and n = 300 low stress). C) STRING-DB

533 association network of signficantly changing, enriched proteins from the low stress salt and/or
534 mannitol conditions. Only nodes with > 2 edges are shown. Increasing line thickness is edge
535 score ranging from 0.5-1. D) Gene ontology biological processes (Benjamini-Hochberg parent-
536 child union) for high stress (left, $p < 0.0025$) and low stress (right, $p < 0.005$) conditions. All
537 proteins enriched in one condition over negative controls were included. Highlighted in red are
538 terms directly related to stress response.

539 **Figure 5. Proteomics data representation of salt and mannitol stressed AHA-treated**
540 **seedlings.** A) PCA plot of high stress (150mM salt - orange and 300mM mannitol - purple) 50µM
541 AHA-treated seedlings, along with control treated (blue) and control untreated (grey) samples.
542 Elipses are 68% confidence; n = 4. B) Same as A but with low stress samples (50mM salt and
543 100mM mannitol). C) Upset plot comparing all protein groups between the AHA-treated whole
544 proteome (8060 proteins), significantly changing proteins in the whole proteome of AHA-treated
545 samples vs. untreated whole proteome (208, > 0.58 Log_2FC and *q-value* < *0.05*), and significantly
546 changing click-enriched proteins from AHA-treated seedlings vs. untreated streptavidin bead
547 binding control (627, > 0.58 Log_2FC and *q-value* < *0.05*); n = 4. D) Comparison of relative
548 methionine content (number of methionine residues over total length of protein) between the
549 entire Arabidopsis proteome from Araport 11 (Proteome) and the 627 significant AHA-tagged
550 proteins enriched (Enriched). Density represents a factor of population size to give the curves
551 equal area.

552 **SUPPLEMENTAL FIGURES**

553 **Supplemental Figure 1. Representative images of seedling samples during AHA and HPG**
554 **viability assays.**

555 **Supplemental Figure 2. Enlarged gene ontology of high stress set AHA-treated seedlings.**

556 **Supplemental Figure 3. Enlarged gene ontology of low stress set AHA-treated seedlings.**

557 **Supplemental Figure 4. Heatmap representation of shared proteins between salt and**
558 **mannitol stressed AHA-treated seedlings.**

559 **Supplemental Figure 5. Comparison of salt and mannitol stress data between previous**
560 **whole proteome analysis and AHA-tagged enrichments.**

561 **Supplemental Figure 6. Gene ontology of salt and mannitol stress data specific to AHA-**
562 **tagged enrichments compared to previous whole proteome analysis.**

563

564 **SUPPLEMENTAL TABLES**

565 **Supplemental Table 1. Enriched AHA-treated low and high salt and mannitol stress**
566 **proteomics data.**

567 **Supplemental Table 2. Differentially expressed proteins above significance threshold**
568 **divided by group between positive control, salt stressed, and mannitol stressed seedlings**
569 **in both high and low stress.**

570 **Supplemental Table 3. Whole proteome data for AHA-treated and untreated proteomes.**

571 **Supplemental Table 4. Comparison of significantly changing proteins in AHA-treated**
572 **stress experiments with significantly changing proteins in stress experiments by**
573 **Rodriguez Gallo et al. (2023)**

574 **Supplemental Table 5. Ontologizer GO output data for AHA-treated low and high salt and**
575 **mannitol stressed proteins.**

576 **Supplemental Table 6. Ontologizer GO output data for AHA-treated stressed proteins that**
577 **are absent from previous whole proteome stress analysis.**

578 **Supplemental Table 7. Methionine proportion analysis raw output data between AHA-**
579 **enriched proteins and the entire Arabidopsis proteome.**

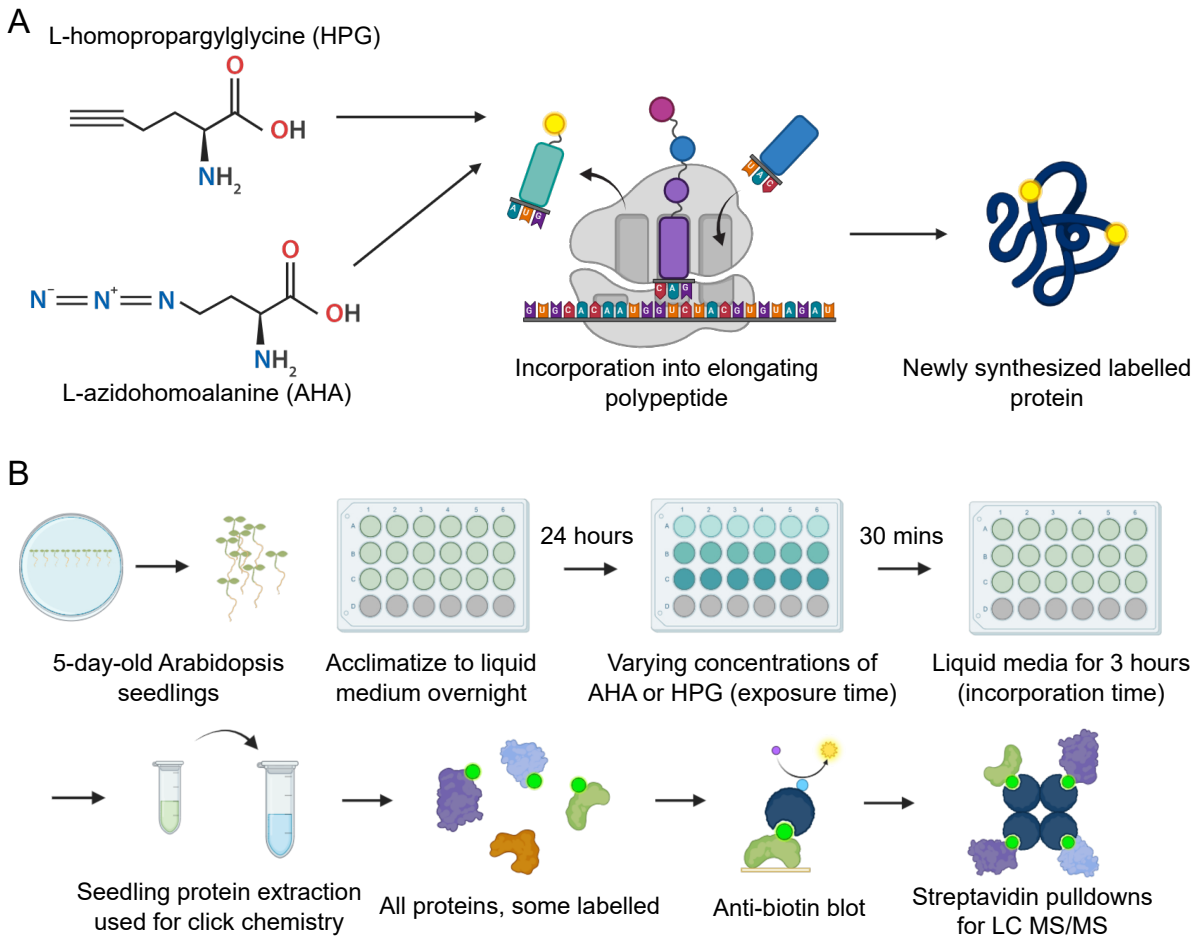

Figure 1. Visualization of BONCAT technology. A) Incorporation mechanism of AHA and HPG into the nascent proteome. B) Workflow for click labelling. Whole seedlings are acclimatized to liquid 0.5X MS media for 24 hours before treatment with AHA or HPG. Acute exposure time in the modified protocol is limited to 30 minutes, followed by 3 hours of incorporation time. Protein is extracted from seedlings for click chemistry in vitro, followed by visualization via anti-biotin blot to determine qualitative labelling before streptavidin enrichment for LC-MS/MS.

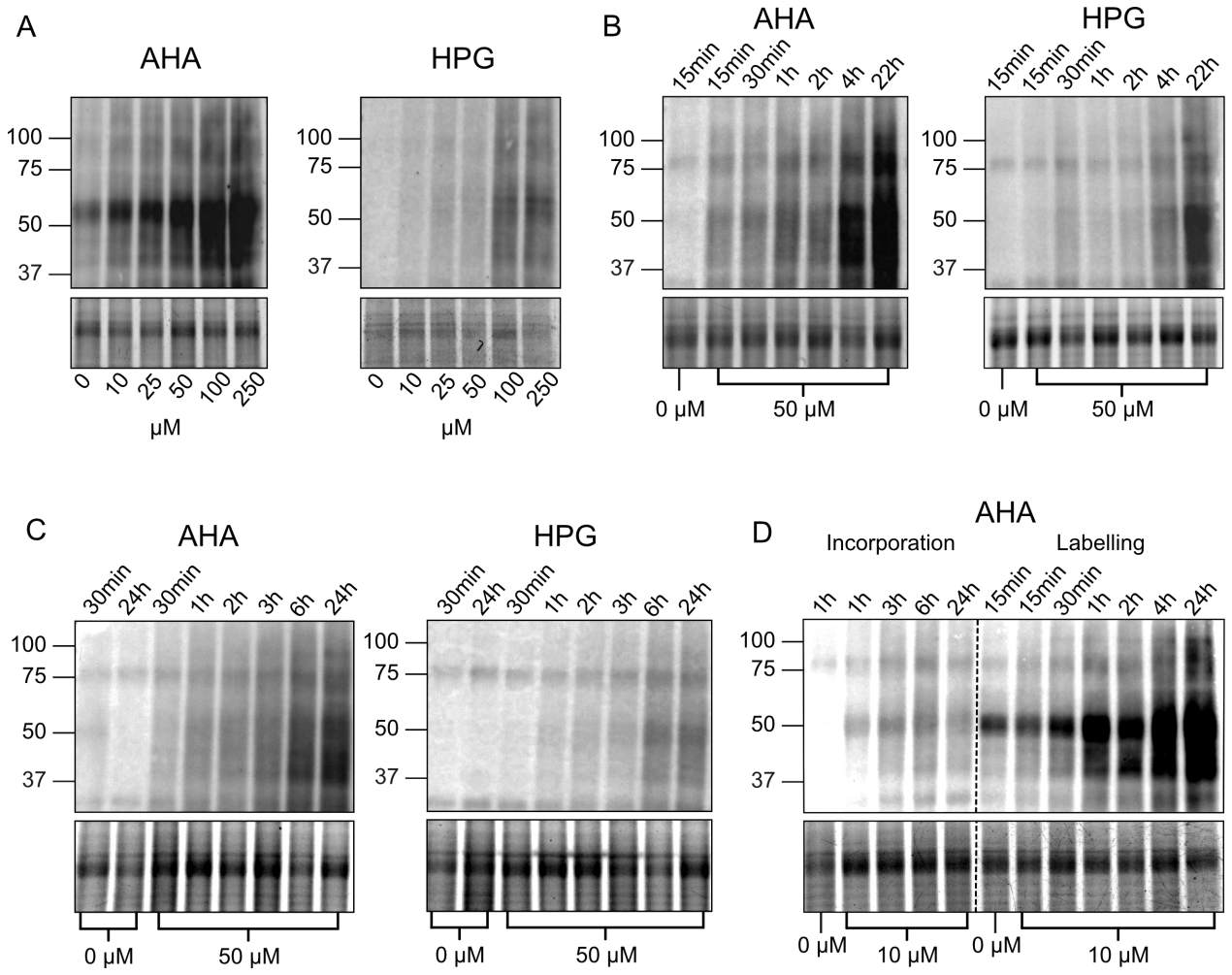

Figure 2. Streptavidin-detected anti-biotin blots of biotin-clicked Arabidopsis whole lysate samples. Beneath each blot is a cropped segment of a Coomassie Blue gel loading control. Each experiment was performed in triplicate, but single replicates are shown for simplicity. A) Titration of AHA and HPG concentrations with a 30-minute acute exposure and 3-hour incorporation time. B) 50μM AHA and HPG tested with exposure times varying from 15 minutes to 22 hours, all followed by a 3-hour incorporation. C) 50μM AHA and HPG tested with incorporation times varying from 30 minutes to 24 hours, each preceded with a 30-minute exposure time. D) Low concentration AHA (10μM) test of varying incorporation times with a 30-minute exposure (left) or varying exposure times with a 3-hour incorporation (right).

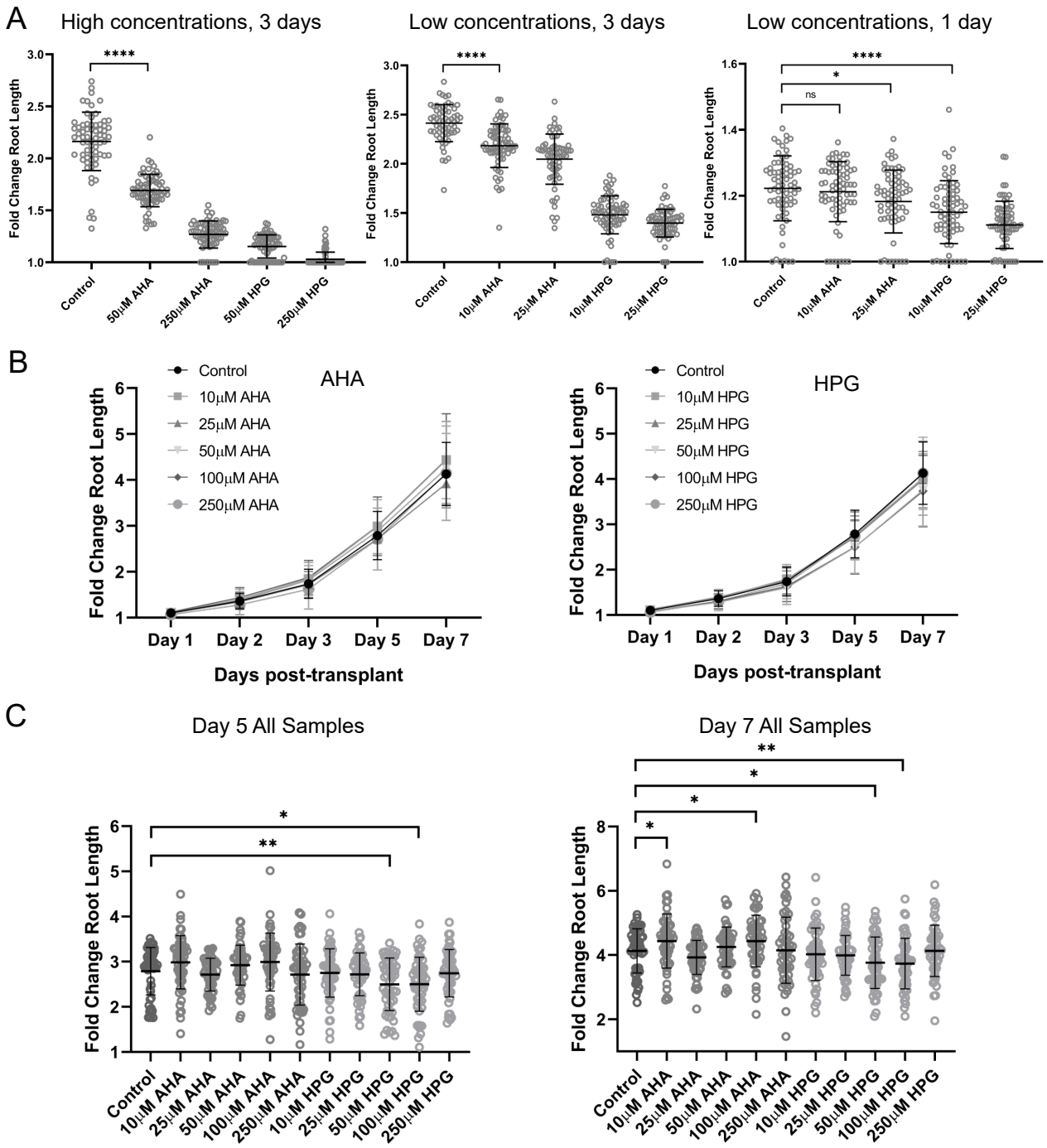

Figure 3. Viability assays of Arabidopsis seedlings exposed to methionine analogs. Average fold change in root length of seedlings with standard deviation error bars is plotted, and t-tests between experimental and control groups were performed with p-value significance < 0.05 shown. A) n = 72 5 d (days)-old seedlings per condition were transplanted to agar plates containing AHA or HPG for 1-3 d to simulate extensive exposure times. High concentrations after 3 days (left), low concentrations after 3 days (middle) and low concentrations after 24 hours (right) are shown. B) n = 54 seedlings per condition were acclimatized to liquid media for 24 h, then exposed for 30 min in AHA- or HPG-containing liquid media before being returned to solid medium and grown for 7 d. C) Snapshot of days 5 and 7 for all conditions from summarized data in 2B to show significant changes.

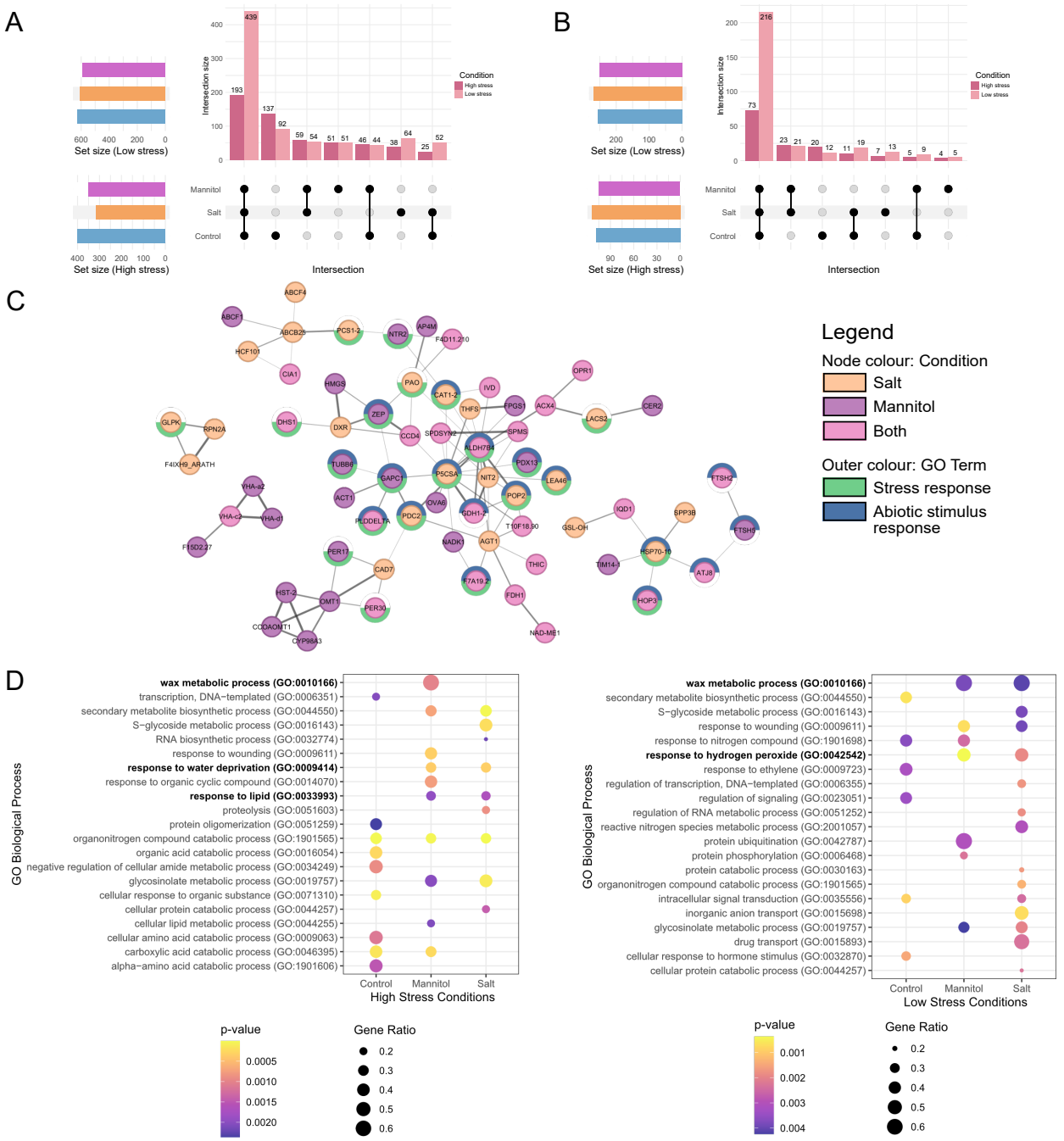

Figure 4. Summary mass spectrometry data for 50µM AHA-labelled 3-hour salt or mannitol stressed Arabidopsis seedlings. A) Upset plot of enriched (>1.5 FC or below detection in negative control) protein groups. Overlaps between positive control (AHA treated, unstressed) and treatment conditions under either 'high stress' (150mM salt and 300mM mannitol, dark, n = 549) or 'low stress' (50mM salt, 100mM mannitol, light, n = 797) conditions are shown. B) Exclusive Class I hits from A that are absent in negative controls (n = 147 high stress and n = 300 low stress). C) STRING-DB association network of signficantly changing, enriched proteins from the low stress salt and/or mannitol conditions. Only nodes with > 2 edges are shown. Increasing line thickness is edge score ranging from 0.5-1. D) Gene ontology biological processes (Benjamini-Hochberg parent-child union) for high stress (left, $p < 0.0025$) and low stress (right, $p < 0.005$) conditions. All proteins enriched in one condition over negative controls were included. Bolded are terms directly related to stress response.

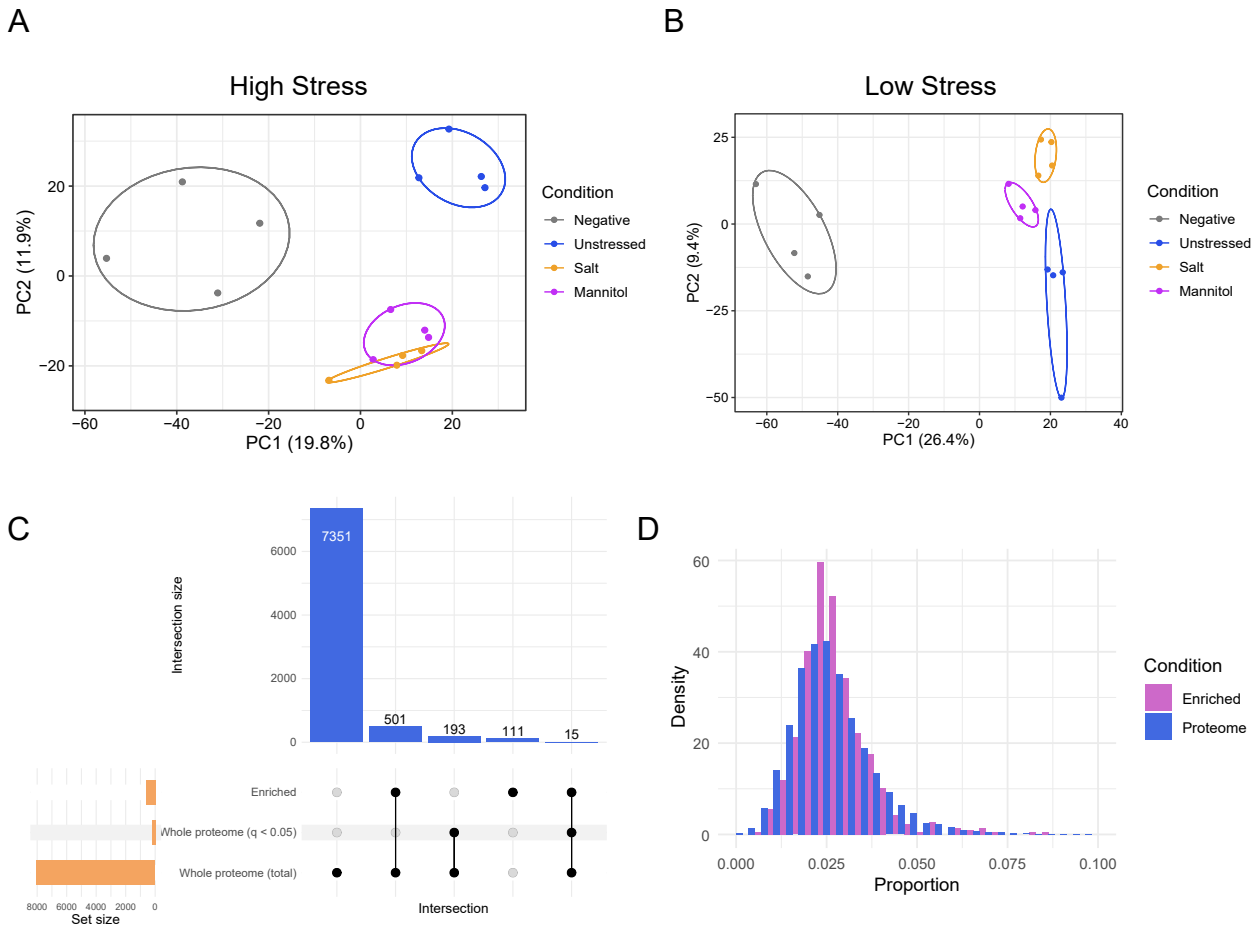

Figure 5. Proteomics data representation of salt and mannitol stressed and unstressed AHA-treated seedlings. A) PCA plot of click enrichments 50µM AHA-treated seedlings under 'high stress' (150mM salt - orange and 300mM mannitol purple) and B) 'low stress' (50mM salt and 100mM mannitol) conditions. Control, AHA-treated (blue) and AHA-untreated (grey) click enrichments are also shown. Elipses are 68% confidence; n = 4. C) Upset plot comparing all protein groups between the AHA-treated whole proteome (8060 proteins), significantly changing proteins in the whole proteome of AHA-treated samples vs. untreated whole proteome (208, > 0.58 Log2FC and q-value < 0.05), and significantly changing click-enriched proteins from AHA-treated seedlings vs. untreated streptavidin bead binding control (627, > 0.58 Log2FC and q-value < 0.05); n = 4. D) Comparison of relative methionine content (number of methionine residues over total length of protein) between the entire Arabidopsis proteome from Araport 11 (Proteome) and the 627 significant AHA-tagged proteins enriched (Enriched). Density represents a factor of population size to give the curves equal area.